Fractals and the Base Eigenvalue of the Laplacian on Certain Noncompact Surfaces

Arthur Baragar

CONTENTS

In this paper, we find bounds on the smallest or base eigenvalue for the Laplacian on the noncompact surfaces within a certain parameterized class. We attempt to fit a curve to the resulting data. These eigenvalues are related to the Hausdorff dimension of certain fractals and to some problems in number theory.

1. BACKGROUND AND ANALYSIS OF THE MAIN RESULT

In the Poincaré disk model of hyperbolic geometry, let us consider the domain $\mathcal{F}$ bounded by the lines AB, AC, and BC', where $A = i$, $B = -i$, $C = e^{i\theta}$, and $C' = e^{-i\theta}$, as shown in Figure 1. Let R_1 be reflection through the line AB, let R_2 be reflection through the line AC, and let R_3 be reflection through the line BC'. Let $\Gamma = \langle R_1, R_2, R_3 \rangle$ be the group of isometries generated by these three maps. Then the image of the domain $\mathcal{F}$ under the action of Γ gives a tiling of the hyperbolic plane $\mathbb{H}^2$, as depicted in Figure 1.

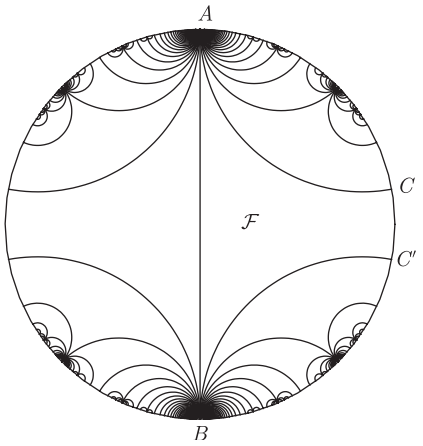

FIGURE 1. A tiling of the plane using reflections and a tile with infinite area (with $\cosh(\gamma/2) = 1.2$).

2000 AMS Subject Classification: Primary 35P15, 37D05, 37F35

Keywords: Minimal eigenvalue, base eigenvalue, Laplacian, Hausdorff dimension, Hecke group, Schottky group

1058-6458/2006 $0.50 per page

The hyperbolic plane modulo the action of Γ forms a noncompact surface $\Gamma\backslash\mathbb{H}^2$ with infinite area. The Laplacian on $\Gamma\backslash\mathbb{H}^2$ has a spectrum of eigenvalues. Of these eigenvalues, the smallest real eigenvalue λ_0 is particularly important, but is a rather mysterious quantity. Several people have devised ways of estimating λ_0, including [Jenkinson and Pollicott 02], [Pignataro and Sullivan 1986], and [McMullen 98].

Two of the angles of the fundamental domain $\mathcal{F}$ are zero. It is possible to define the "intersection" of the two lines AC and BC'. This intersection occurs off the plane and defines an imaginary angle $i\gamma$, which is preserved under isometries. Our main result is the following:

Theorem 1.1. *Let $\Gamma = \langle R_1, R_2, R_3\rangle$ be a group of isometries of $\mathbb{H}^2$ generated by the reflections R_1, R_2, and R_3, which are reflections through the lines AB, AC, and BC', respectively. Let the angles at A and B be zero, and let the angle between the lines AC and BC' be $i\gamma$, where γ is real. Then the smallest eigenvalue λ_0 for the Laplacian acting on the surface $\Gamma\backslash\mathbb{H}^2$ has the bounds shown in Table 1.*

The hope is that by looking at a parameterized set of values, it might be possible to find a function that fits the data and that knowing this function might give us some insight as to the actual value of λ_0.

The hyperbolic plane has a natural compactification with the unit circle. For a point P in $\mathbb{H}^2$, define the *limit set* $\Lambda(\Gamma)$ for Γ to be the closure of $\Gamma(P)$ in the compactification of $\mathbb{H}^2$. This set is in the unit circle $\mathbb{S}^1$, is independent of the choice for P, and is often a Cantor-like fractal. Let α be the Hausdorff dimension for $\Lambda(G)$. Then, by a result due to Lax and Phillips [Lax and Phillips 82], α and λ_0 are related by

$$\lambda_0 = \alpha(1-\alpha).$$

We will find bounds on λ_0 by finding bounds on α.

There is another way of visualizing the Cantor-like character of the limit set $\Lambda(\Gamma)$. Let DD' be a mutual orthogonal of the lines AC and BC', and let P be a point on DD'. It is clear that repeated applications of combinations of R_2 and R_3 will keep the image of P on DD', while all other elements of Γ will move P to a point to the "left" of DD' in Figure 2. The limit set $\Lambda(\Gamma)$ therefore includes the points D and D', but does not include any points on the arc "cut out" by DD'. The image of DD' under the action of an element of Γ generates another arc with the same property. The limit set $\Lambda(\Gamma)$ is the portion of $\mathbb{S}^1$ that is left after all these arcs are removed. It is clear that this set is uncountable and has measure zero.

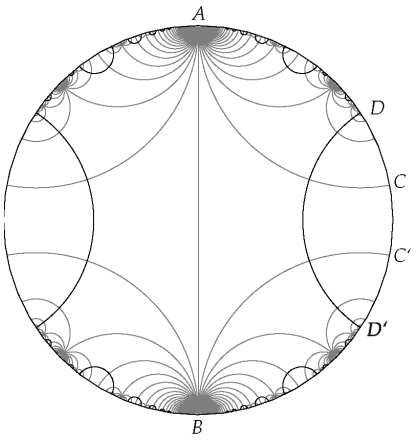

FIGURE 2. A visualization of the Cantor-like nature of the limit set $\Lambda(\Gamma)$. The limit set is the set of points on the unit disk $\mathbb{S}^1$ that are "outside" all images of DD' under the action of Γ.

The idea of studying a parameterized set of eigenvalues is not new. Both Phillips and Sarnak [Phillips and Sarnak 85a], and McMullen [McMullen 98] have studied similar classes. Phillips and Sarnak look at the Hecke group

$$\Gamma_\mu = \left\langle z + 2\mu, \frac{-1}{z} \right\rangle$$

acting on the Poincaré upper-half-plane model of $\mathbb{H}^2$. The map $z \mapsto z + 2\mu$ is a parabolic translation centered at ∞, and the map $z \mapsto -1/z$ is rotation by π about the point i. Fundamental domains in the Poincaré upper-half-plane and disk models are shown in Figure 3. A fundamental domain for the Hecke group can be made the same as the fundamental domain $CABC'$ for our group if $\mu = \cosh(\gamma/2)$. Though the groups are different, it is clear that their limit sets are equal, so their base eigen-

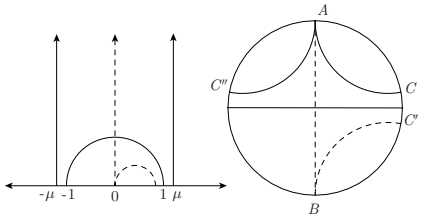

FIGURE 3. Two fundamental domains for the Hecke group. In the disk model, the map $z \mapsto -1/z$ is rotation by π about the origin, and the map $z \mapsto z + 2\mu$ is the parabolic translation with fixed point A that translates C'' to C. Using the fundamental domain $CABC'$, the Hecke group generates the same tiling as in Figure 1.

a	Lower bound	Upper bound
1.1	.087	.110
1.11	.092	.114
1.2	.129	.142
1.25	.143	.153
1.3	.1552	.1624
1.4	.1723	.1770
1.5	.1846	.1879
1.6	.1940	.1964
1.7	.2012	.2030
1.8	.2071	.2085
1.9	.2118	.2129
2	.21588	.21659
2.1	.21919	.21975
2.2	.22201	.22246
2.3	.22443	.22480
$\sqrt{11/2}$	.22541	.22576
2.4	.22653	.22683
2.5	.22836	.22861
2.7	.23140	.23157
3	.23482	.23493
3.5	.238665	.238715
4	.241158	.241186
4.5	.242880	.242897
5	.244126	.244139
6	.2457802	.2457844
7	.2468052	.2468072
8	.2474884	.2474896
9	.24796870	.24796927
10	.24832018	.24832054
11	.24858577	.24858600
12	.24879171	.24879186
13	.24895484	.24895495
14	.249086407	.249086474
15	.249194152	.249194203
16	.249283570	.249283607

a	Lower bound	Upper bound
17	.249358639	.249358668
18	.249422309	.249422331
19	.249476800	.249476817
20	.249523813	.249523828
25	.2496844592	.2496844637
30	.2497750952	.2497750973
35	.2498313709	.2498313719
40	.24986876207	.24986876260
45	.24989489537	.24989489568
50	.24991389227	.24991389246
60	.249939110053	.249939110135
70	.249954640664	.249954640706
80	.249964888568	.249964888591
90	.249972008675	.249972008690
100	.2499771579283	.2499771579373
120	.2499839510069	.2499839510111
140	.2499881046330	.2499881046352
160	.2499908295937	.2499908295951
180	.24999271384298	.24999271384379
200	.24999407107076	.24999407107131
250	.24999617263584	.24999617263608
300	.24999732598070	.24999732598082
350	.249998026555899	.249998026556027
400	.249998483803527	.249998483803561
450	.249998798671908	.249998798671930
500	.249999024698102	.249999024698117
600	.2499993203118967	.2499993203119041
700	.2499994993332486	.2499994993332533
800	.2499996159053168	.2499996159053204
900	.2499996960313681	.2499996960313715
1000	.2499997534632639	.2499997534632677
1250	.2499998418339495	.2499998418339532
1667	.2499999108419694	.2499999108419730
2500	.2499999602524740	.2499999602524774
5000	.2499999900344118	.2499999900344140

TABLE 1. A table of lower and upper bounds on λ_0 as a function of the parameter $a = \cos(i\gamma/2) = \cosh(\gamma/2)$.

values are equal. They study λ_0 as a function of μ, and come up with a graph similar to the ones in Figures 4 and 5. Their study of λ_0 is also via the Hausdorff dimension α, using the result of Lax and Phillips [Lax and Phillips 82] that

$$N(P, O, T) \sim cT^{\alpha},$$

where c depends on P and O, α is independent of the choices for P and O, and

$$N(P, O, T) = \#\{Q \in \Gamma_\mu(P) : \cosh|OQ| < T\}.$$

The quantity $|OQ|$ is the hyperbolic distance between O and Q, so $N(P, O, T)$ is the number of points in the orbit of P that lie in the disk centered at O with radius $\operatorname{arccosh} T$. The error terms stated in the paper [Phillips and Sarnak 85a] are estimates, and strike this author as being somewhat bold (based on the method used), though they are correct. Phillips and Sarnak prove several properties of the graph in Figures 4 and 5. They prove that it is continuous and increasing [Phillips and Sarnak 85b], and that it is concave down [Phillips and Sarnak 85a].

An example studied by McMullen in [McMullen 98] is also closely related to our class. He studied the group in the Poincaré upper-half-plane model of $\mathbb{H}^2$ generated by reflections in the lines whose endpoints are $\{\infty, -1\}$, $\{\infty, 1\}$, and $\{-r, r\}$. He notes that the limit set for this group is the same as the limit set for the Hecke group Γ_μ for $\mu = 1/r$. He proves that

$$\alpha = \frac{1+r}{2} + O(r^2),$$

from which we conclude that

$$\lambda_0 = \frac{1-r^2}{4} + O(r^3). \tag{1–1}$$

Since $r = \operatorname{sech}(\gamma/2)$, this implies that, asymptotically,

$$\lambda_0 \sim \frac{\tanh^2(\gamma/2)}{4}. \tag{1–2}$$

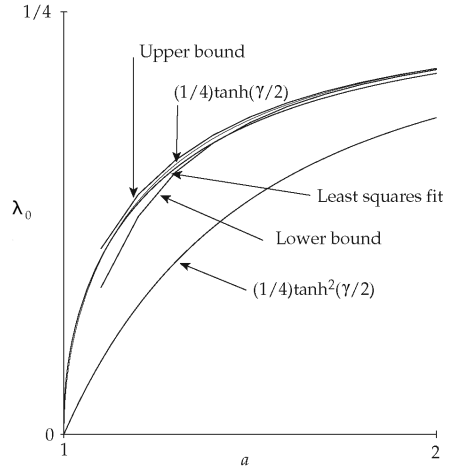

FIGURE 4. A graph of λ_0 as a function of $a = \cosh(\gamma/2)$ over the domain $a \in [1, 2]$, together with the graphs of $\frac{1}{4}\tanh^2(\gamma/2)$, $\frac{1}{4}\tanh(\gamma/2)$, and the function $\frac{1}{4}\tanh(.4733\gamma + .0264)$, which was found using a least squares fit of the curve in Figure 8.

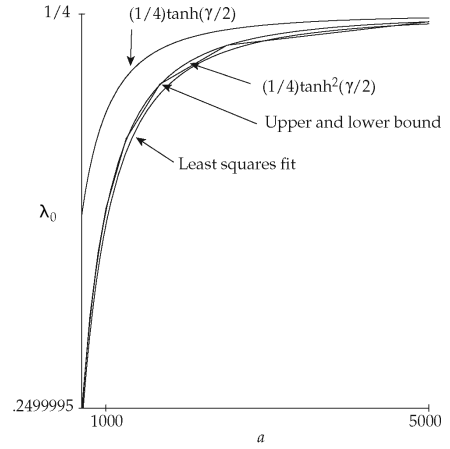

FIGURE 5. The same graph as in Figure 4, but with $a \in [700, 5000]$.

The graph of $y = \frac{1}{4}\tanh^2(\gamma/2)$ is also included in Figures 4 and 5. Rearranging (1–1), we get

$$a = \frac{1}{r} \sim \frac{1}{\sqrt{1 - 4\lambda_0}},$$

which suggests that we look at the graph of $1/\sqrt{1 - 4\lambda_0}$ as a function of a; see Figure 6. The expansion (1–1) can also be thought of as a Taylor expansion for λ_0 expanded about $r = 0$. In an effort to estimate the coefficient of the cubic term, we are led to investigate $(\lambda_0 - \frac{1}{4}\tanh^2(\gamma/2))^{-1/3}$ as a function of a, which is shown in Figure 7. Though this graph is fairly linear, it is not linear enough for one to confidently guess the appropriate slope.

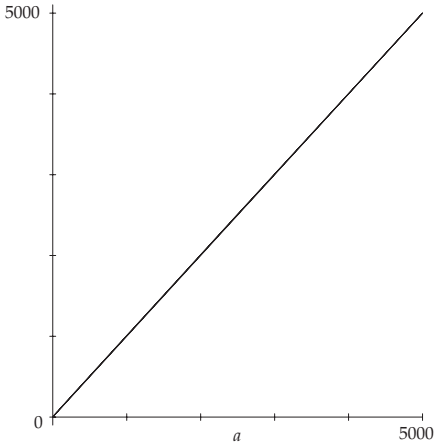

FIGURE 6. The graph of $1/\sqrt{1 - 4\lambda_0}$ (using both the upper and lower bounds) together with $y = x$ (yes, they are all there).

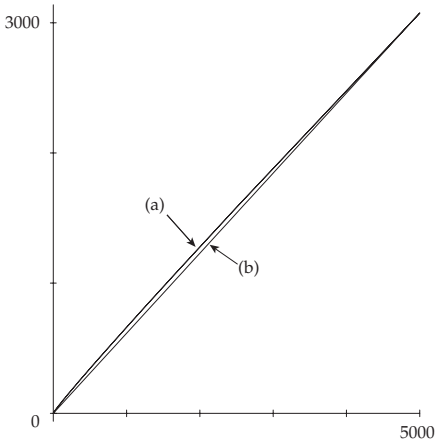

FIGURE 7. The graph of (a) the curve $(\lambda_0 - \tanh^2(\gamma/2)/4)^{-1/3}$ and (b) the line $y = .615x$. The upper and lower bounds for λ_0 are included in both graphs. They are not sufficiently different to distinguish them.

McMullen also shows that as r approaches 1 (from the left), λ_0 is bounded above and below by constant multiples of $\sqrt{1 - r}$. For small a, we find the intriguing empirical approximation

$$\lambda_0 \approx \frac{\sqrt{a^2 - 1}}{4a} = \frac{1}{4}\tanh(\gamma/2). \qquad (1\text{–}3)$$

The graph of this function is also included in Figures 4 and 5. For a near 1, this gives the approximation

$$\lambda_0 \approx \frac{\sqrt{2}}{4}\sqrt{1 - r},$$

which is consistent with McMullen's result.

The asymptotic formula in (1–2) and the approximation in (1–3) suggest that we look at $\operatorname{arctanh}(2\sqrt{\lambda_0})$

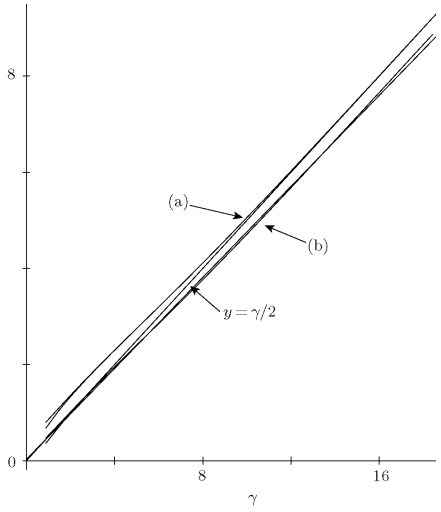

FIGURE 8. A plot of $y = \gamma/2$ together with (a) $\operatorname{arctanh}(2\sqrt{\lambda_0})$ as a function of γ, and (b) $\operatorname{arctanh}(4\lambda_0)$ as a function of γ. Note that the line $y = \gamma/2$ is a good approximation to (a) for large γ, reflecting the asymptotic relation $\lambda_0 \sim \tanh^2(\gamma/2)$, while it is a good approximation to (b) for small γ, suggesting the approximation $\lambda_0 \approx \tanh(\gamma/2)$ near zero. The least squares fit to (b) is also shown.

and $\operatorname{arctanh}(4\lambda_0)$ as functions of γ, graphs that can be thought of as analogues of a log-log graph. These graphs, shown in Figure 8, are also fairly linear. A least squares fit to $\operatorname{arctanh}(4/\lambda_0)$ is included to illustrate how linear these graphs are. The least squares fit gives the approximation $g(\cosh(\gamma/2)) \approx \frac{1}{4}\tanh(.4733\gamma + .0264)$, which is also shown in Figures 4 and 5. Though it is, in places, a better fit than either of the other two approximations, it

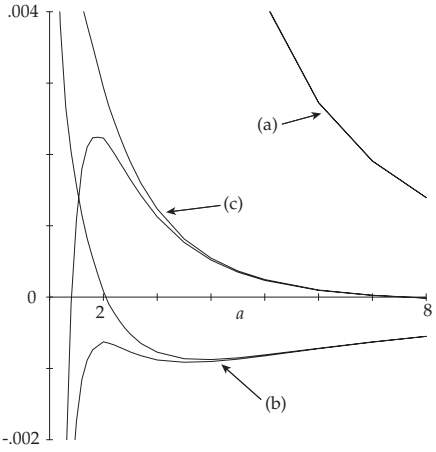

FIGURE 9. A graph of the differences between the various fits and the upper and lower bounds for λ_0, for (a) $\frac{1}{4}\tanh^2(\gamma/2)$; (b) $\frac{1}{4}\tanh(\gamma/2)$; and (c) the least squares fit.

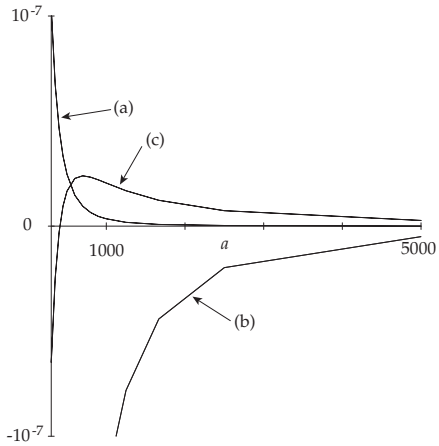

FIGURE 10. The same graph as in Figure 9, but with $a \in [0, 5000]$.

fails to go through 0 when $\gamma = 0$, and probably will not do much for our objective of evoking insight.

Finally, in Figures 9 and 10, we show the difference between the bounds and the various fits we have discussed so far. Though the graphs seem rather simple, nothing nice dreamt up by the author fit them very well.

2. THE LORENTZ MODEL

Our algorithm and understanding of the angle γ depend on the Lorentz model of $\mathbb{H}^2$. Lorentz space, denoted by $\mathbb{R}^{2,1}$, is three dimensions equipped with the Lorentz product $\mathbf{x} \odot \mathbf{y} = \mathbf{x}^t J \mathbf{y}$, where

$$J = \begin{bmatrix} 1 & 0 & 0 \\ 0 & 1 & 0 \\ 0 & 0 & -1 \end{bmatrix}.$$

The equation $\mathbf{x} \odot \mathbf{x} = -1$ describes a hyperboloid of two sheets, and the sheet with $x_3 > 0$ is a model of $\mathbb{H}^2$ (where $\mathbf{x} = (x_1, x_2, x_3)$). The distance between two points P and Q in $\mathbb{H}^2$ is given by $P \odot Q = -\cosh|PQ|$. A line on $\mathbb{H}^2$ is the set of points $\mathbf{x} \in \mathbb{H}^2$ that satisfies $\mathbf{n} \odot \mathbf{x} = 0$, where $\mathbf{n} \odot \mathbf{n} = 1$. The angle θ between two lines $\mathbf{n} \odot \mathbf{x} = 0$ and $\mathbf{m} \odot \mathbf{x} = 0$ is given by $\mathbf{n} \odot \mathbf{m} = \cos\theta$. This angle is real if the lines intersect in $\mathbb{H}^2$, and imaginary otherwise. The group

$$\mathcal{O} = \{T \in M_{3\times 3}(\mathbb{R}) : T^t J T = J\}$$

preserves the Lorentz product. That is, $(T\mathbf{x}) \odot (T\mathbf{y}) = \mathbf{x} \odot \mathbf{y}$ for all $T \in \mathcal{O}$. The subgroup $\mathcal{O}^+$ that sends $\mathbb{H}^2$ to itself is the group of isometries on $\mathbb{H}^2$. It is clear that an element of $\mathcal{O}^+$ preserves both angles and distance, since it preserves the Lorentz product. The projection of $\mathbb{H}^2$ through the point $(0, 0, -1)$ and onto the plane $x_3 = 0$ is a

projection of $\mathbb{H}^2$ onto the Poincaré disk model. The point A in Figure 1 therefore has coordinates $(0,1,1)$ in Lorentz space. Since this point is at infinity, its representation is not unique. The point B has coordinates $(0,-1,1)$; the point $C = (\cos\theta, \sin\theta, 1)$; and $C' = (\cos\theta, -\sin\theta, 1)$. It is clear that the line AB has the equation $\mathbf{n}_1 \odot \mathbf{x} = 0$, where $\mathbf{n}_1 = (1,0,0)$. To find the equations of AC and BC', we use the Lorentz cross product, which is given by $\mathbf{x} \otimes \mathbf{y} = J^{-1}(\mathbf{x} \times \mathbf{y})$. This vector is perpendicular to both $\mathbf{x}$ and $\mathbf{y}$ (with respect to the Lorentz product). Thus the normal to AC is $\mathbf{n}_2 = (1,a,a)$, where $a = \frac{\cos\theta}{1-\sin\theta}$, and the normal to BC' is $\mathbf{n}_3 = (1,-a,a)$. Note that the projection of $\mathbf{x}$ onto $\mathbf{n}$ is given by $(\mathbf{n} \odot \mathbf{x})\mathbf{n}$ (since $\mathbf{n} \odot \mathbf{n} = 1$), so the reflection of $\mathbf{x}$ through the line with normal $\mathbf{n}$ is $\mathbf{x} - 2(\mathbf{n} \odot \mathbf{x})\mathbf{n}$. Thus, the reflections R_i have the matrix representations

$$R_1 = \begin{bmatrix} -1 & 0 & 0 \\ 0 & 1 & 0 \\ 0 & 0 & 1 \end{bmatrix}, \quad R_2 = \begin{bmatrix} -1 & -2a & 2a \\ -2a & 1-2a^2 & 2a^2 \\ -2a & -2a^2 & 1+2a^2 \end{bmatrix},$$

and

$$R_3 = \begin{bmatrix} -1 & 2a & 2a \\ 2a & 1-2a^2 & -2a^2 \\ -2a & 2a^2 & 1+2a^2 \end{bmatrix}.$$

The imaginary angle $i\gamma$ between the lines AC and BC' is given by $\cos(i\gamma) = \cosh(\gamma) = -\mathbf{n}_2 \odot \mathbf{n}_3 = 2a^2 - 1$. Since $a > 1$, we have $\cosh(\gamma) > 1$ and hence γ is real. By the double angle formula, we have $a = \cos(i\gamma/2) = \cosh(\gamma/2)$.

The author's interest in these sorts of problems arose out of the study of K3 surfaces. Let V be an algebraic K3 surface defined over a number field K. The Picard group $\mathrm{Pic}(V)$ is a lattice in $\mathbb{R}^n$, where n is the Picard number and $1 \le n \le 20$. The intersection pairing on $\mathrm{Pic}(V)$ is a Lorentz inner product. The group $\mathrm{Aut}(V)$ of automorphisms on V maps naturally into a discrete subgroup of isometries Γ of $\mathrm{Pic}(V)$. If there are any -2 curves on V, then the fundamental domain for Γ is infinite, and we have an analogous situation. The dimension α is a measure of the asymptotic growth of the number of curves in the orbit of a base curve under the action of $\mathrm{Aut}(V)$. In [Baragar 03], this problem was studied for a particular class of K3 surfaces with Picard number three. The fundamental domain for that example is the same as that shown in Figure 1, with an imaginary angle $i\gamma$ that satisfies $a = \cosh(\gamma/2) = \sqrt{11/2}$. The group Γ includes the reflections R_2 and R_3, but instead of a reflection across AB, Γ includes a rotation by π about a point $P = (3-2\sqrt{2})i$ on the line AB. Figure 11 shows how this change affects the tiling. The eigenvalue λ_0 for this

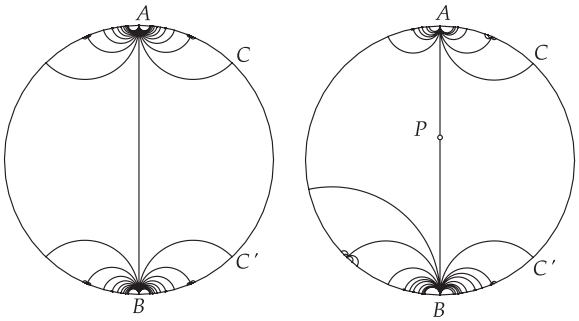

FIGURE 11. The tiling induced by $\Gamma = \langle R_1, R_2, R_3 \rangle$ with $a = \sqrt{11/2}$ (left), and the tiling induced by $\Gamma = \langle S_P, R_2, R_3 \rangle$ with $a = \sqrt{11/2}$ and the rotation S_P by π about $P = i(3-2\sqrt{2})$ (right).

group is not expected to be the same as the one using a reflection, though by a result due to Phillips and Sarnak [Phillips and Sarnak 85b], we know that it is no smaller. Indeed, in [Baragar 03], we find $\lambda_0 = .22670 \pm .00035$, while using a reflection, we obtain $\lambda_0 = .22558 \pm .00018$.

The mutual orthogonal DD' to AC and AC' and its image under the action of Γ have special meanings within the Picard group. The line DD' represents a -2 curve. The interior of its image under the action of Γ, shown in Figure 12, also tiles the plane under the action of the group generated by reflection through $\sigma(DD')$ for all $\sigma \in \Gamma$. One of these tiles contains an ample divisor. That tile is a hyperbolic cross section of the Kähler or ample cone. That is, if P represents an ample divisor, and we intersect the ample cone with the surface $\mathbf{x} \odot \mathbf{x} = 1$, then

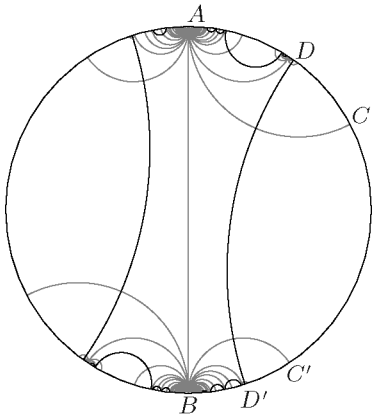

FIGURE 12. The same tiling as in Figure 11, but with the center of the rotation at the origin (light lines), together with the image of the mutual orthogonal DD' under the action of Γ (dark lines). The open region that includes the origin and is bounded by the dark lines is a hyperbolic cross section for the ample cone for a class of K3 surfaces.

the resulting region is the one shown in Figure 12. An alternative cross section to take is a Euclidean cross section. If we intersect the ample cone with a plane away from the origin and orthogonal to the center of the rotation S_P, we get the Beltrami–Klein model for the same region. That is the region derived from Figure 12, where the endpoints of the arcs of the circles are joined with Euclidean line segments.

3. THE ALGORITHM

Let us define the height

$$h(P) = P_3$$

for $P = (P_1, P_2, P_3)$. Since $-O \odot P = P_3$ for $O = (0, 0, 1)$, the height is related to the hyperbolic distance by $h(P) = \cosh |OP|$, and hence

$$N(P, O, T) = \#\{Q \in \Gamma(P) : h(Q) \leq T\}.$$

Let

$$\alpha = \lim_{T \to \infty} \frac{\log(N(P, O, T))}{\log T}.$$

Then α exists, and is related to λ_0 by the result in [Lax and Phillips 82] cited earlier: $\lambda_0 = \alpha(1 - \alpha)$. Our study of λ_0 is through the study of α. Let

$$f(s, P) = \sum_{\sigma \in \Gamma} (h(\sigma P))^{-s}.$$

It is known that $f(s, P)$ converges for $s > \alpha$ and diverges for $s < \alpha$. The boundary of convergence is independent of $P \in \mathbb{H}^2$.

Because the group $\Gamma = \langle R_1, R_2, R_3 \rangle$ is isomorphic to $\mathbb{Z}/2\mathbb{Z} * \mathbb{Z}/2\mathbb{Z} * \mathbb{Z}/2\mathbb{Z}$, there exists a unique *minimal representation* for $\sigma \in \Gamma$ such that $\sigma = R_{k_m} \cdots R_{k_1}$ with $k_i \neq k_{i+1}$ for $i = 1, \ldots, m - 1$. Let us call m the *length* of σ and write $l(\sigma) = m$.

The group Γ also has a natural tree structure whose nodes are elements $\sigma \in \Gamma$ and whose edges are pairs $\{\sigma, R_i\sigma\}$. A subset U of Γ is a subtree if it is connected. We will be particularly interested in the subtrees

$$U_i = \{\sigma \in \Gamma : l(\sigma R_i) \geq l(\sigma)\}.$$

These are the elements of Γ whose minimal representations do not end with R_i. Let

$$f_i(s, P) = \sum_{\sigma \in U_i} (h(\sigma P))^{-s}.$$

The tree structure on Γ induces a natural tree structure on orbits. We will say that a point $X \in \Gamma(P)$ *descends* to σX if $h(\sigma X) < h(X)$ and $\sigma \in \{R_2, R_3, R_2R_1, R_3R_1\}$. We will say that σ gives *descent* from X.

Lemma 3.1. *Suppose $X = (x, y, z)$ satisfies $X \odot X = 0$ and that $h(X) > 0$. Suppose that σ and τ are distinct elements in $\{R_2, R_3, R_2R_1, R_3R_1\}$, and that σ gives descent from X. Then $h(\tau X) > h(X)$.*

Proof: The quantity $h(\rho X) - h(X)$ for each of $\rho \in \{R_2, R_3, R_2R_1, R_3R_1\}$ is one of

$$(1 + a^2)z \pm 2ax \pm 2a^2y,$$

for one of the four combinations of signs. Let us first suppose that $x, y \geq 0$. Since σ gives descent, we may assume that it is the ρ that makes both signs negative. Suppose then that there exists a $\tau \neq \sigma$ such that $h(\tau X) \leq h(X)$. Then either

$$(1 + a^2)z \leq 2ax - 2a^2y \tag{3–1}$$

or

$$(1 + a^2)z \leq -2ax + 2a^2y. \tag{3–2}$$

If we have (3–1), then

$$2a^2z < (1 + 2a^2)z \leq 2ax,$$
$$z < x/a < x.$$

But $x^2 + y^2 - z^2 = 0$ so $z \geq x$, a contradiction. Similarly, from (3–2), we get $z < y$. Thus, $h(\tau X) > h(x)$ for all $\tau \neq \sigma$.

By symmetry, the same argument works for the other three combinations of $\pm x, \pm y \geq 0$. □

Corollary 3.2. *For any $\sigma \in \Gamma$, we have $h(\sigma A) > 0$, $h(\sigma B) > 0$, $h(\sigma C) > 0$, and $h(\sigma C') > 0$.*

Proof: We first observe that $A \odot A = B \odot B = C \odot C = C' \odot C' = 0$, so Lemma 3.1 applies.

We note that $h(A) = 1$ and that $R_1A = R_2A = A$. We note that $R_3A = (4a, 1-4a^2, 1+4a^2)$, so R_3 gives descent from R_3A. Using induction on the length of $\sigma \in U_3$ and the above lemma, we conclude that $h(\sigma R_3 A) > 0$ for all $\sigma \in U_3$. Thus $h(\sigma A) > 0$ for all $\sigma \in \Gamma$. By symmetry, $h(\sigma B) > 0$ for all $\sigma \in \Gamma$.

Similarly, we note that $h(C) = 1$; that $R_2C = C$; that $h(R_3C) = 1+4a^2 \sin\theta > 1$, $h(R_2R_1C) = 1+4a\cos\theta > 1$; and that $h(R_3R_1C) = 1 + 4a^2 > 1$. We use induction on the length of $\sigma \in U_3$ to show that $h(\sigma R_3 C) > 0$ and $h(\sigma R_3 R_1 C) > 0$, and induction on the length of $\sigma \in U_2$ to show that $h(\sigma R_2 R_1 C) > 0$. Thus, $h(\sigma C) > 0$ for all $\sigma \in \Gamma$. By symmetry, $h(\sigma C') > 0$ for all $\sigma \in \Gamma$. □

Lemma 3.3. *Suppose $X = (x, y, z)$ satisfies $X \odot X = 1$ and that $h(X) \geq a$. Suppose that σ and τ are distinct elements in $\{R_2, R_3, R_2R_1, R_3R_1\}$, and that σ gives descent from X. Then $h(\tau X) > h(X)$.*

Proof: As in the proof of Lemma 3.1, let us first suppose that $x, y \geq 0$. If there exists a $\tau \neq \sigma$ such that $h(\tau X) \leq h(X)$, then we have either (3–1) or (3–2) from the proof of Lemma 3.1. If we have (3–1), then

$$\begin{aligned}(1+2a^2)z &\leq 2ax,\\ (1+2a^2)^2z^2 &\leq 4a^2x^2 \leq 4a^2(z^2+1),\\ (1+4a^4)z^2 &\leq 4a^2,\\ z^2 &\leq \frac{4a^2}{1+4a^4} < \frac{1}{a^2} < a^2,\\ z &< a.\end{aligned}$$

In the above, we used that $x^2+y^2-z^2 = 1$, so $x^2 \leq z^2+1$. If we have (3–2), then

$$\begin{aligned}(1+2a^2)z &\leq 2a^2y,\\ (1+2a^2)^2z^2 &\leq 4a^4(z^2+1),\\ (1+4a^2)z^2 &\leq 4a^4,\\ z^2 &\leq \frac{4a^4}{1+4a^2} < a^2,\\ z &< a.\end{aligned}$$

Now argue as in the proof of Lemma 3.1. □

Corollary 3.4. *For any $\sigma \in U_3$, we have*

$$h(\sigma \mathbf{n}_3) = h(\sigma(1, -a, a)) > 0.$$

Proof: Note that $R_3(1, -a, a) = (-1, a, -a)$, so R_3 gives descent. □

These corollaries give us a type of self-similarity statement:

Lemma 3.5. *Let $X = (x, y, z)$. If $x, y, z > 0$ and $ax + y - z > 0$, then*

$$\begin{aligned}&\left(\frac{y+z}{2}\right)^{-s} f_3(s, T_3A)\\ &\quad< f_3(s, T_3X)\\ &\quad< \left(\frac{y+z}{2} - \frac{2ax+y-z}{2a^2}\right)^{-s} f_3(s, T_3A).\end{aligned}$$

If $x < 0$, $y, z > 0$, and $ax + y - z < 0$, then

$$\begin{aligned}&\left(\frac{y+z}{2} - \frac{2ax+y-z}{2a^2}\right)^{-s} f_3(s, T_3A)\\ &\quad< f_3(s, T_3X)\\ &\quad< \left(\frac{y+z}{2}\right)^{-s} f_3(s, T_3A).\end{aligned}$$

The series $f_3(s, T_3A)$ will play a central role in our argument, so let us define $f(s) = f_3(s, T_3A)$.

Proof: Writing X as a linear combination of A, B, and $-\mathbf{n}_3$, we get

$$X = \frac{y+z}{2}(0, 1, 1) - \frac{ax+y-z}{2}(0, -1, 1) - x(-1, a, -a),$$

so if $x > 0$ and $ax + y - z > 0$, then for all $\sigma \in U_3$,

$$\begin{aligned}h(\sigma R_3 X) &< \frac{y+z}{2} h(\sigma R_3 A),\\ h(\sigma R_3 X)^{-s} &> \left(\frac{y+z}{2}\right)^{-s} h(\sigma R_3 A)^{-s},\\ f_3(s, R_3X) &> \left(\frac{y+z}{2}\right)^{-s} f_3(s, R_3A) = \left(\frac{y+z}{2}\right)^{-s} f(s).\end{aligned}$$

Similarly, if $ax + y - z < 0$ and $x < 0$, then

$$f_3(s, R_3X) < \left(\frac{y+z}{2}\right)^{-s} f(s).$$

Writing X as a linear combination of A, C', and $-\mathbf{n}_3$, we get

$$\begin{aligned}X = &\left(\frac{y+z}{2} - \frac{2ax+y-z}{2a^2}\right) A + \frac{2ax+y-z}{a\cos\theta} C'\\ &+ \frac{ax+y-z}{a}(-\mathbf{n}_3).\end{aligned}$$

Thus, if $x > 0$ and $ax + y - z > 0$, then $2ax + y - z > 0$ and

$$f_3(s, R_3X) < \left(\frac{y+z}{2} - \frac{2ax+y-z}{2a^2}\right)^{-s} f(s).$$

And if $x < 0$ and $ax + y - z < 0$, then $2ax + y - z < 0$ and

$$f_3(s, R_3X) > \left(\frac{y+z}{2} - \frac{2ax+y-z}{2a^2}\right)^{-s} f(s).$$

□

Note that if R_2 gives descent from X with $h(X) > 0$, then $x, y, z > 0$ and $x/a + y - z > 0$, so $ax + y - z > 0$.

Also, if R_2R_1 gives descent from X with $h(X) > 0$, then $x < 0$, $y, z > 0$, and $x/a + y - z < 0$, so $ax + y - z < 0$.

Corollary 3.6. *The series $f(s) = f_3(s, R_3A)$ converges for all $s > \alpha$ and diverges for all $s < \alpha$.*

Proof: Let us compare $f(s)$ with $f(s, O)$, where $O = (0, 0, 1)$. Note that $R_1O = O$, $R_2O = (-2a, -2a^2, 1 + 2a^2)$, and $R_3O = (-2a, 2a^2, 1 + 2a^2)$. By symmetry, $f_2(s, R_2O) = f_3(s, R_3O) = f(s)$, so

$$f(s, O) = 1 + 4f(s).$$

For $X = R_3O$, we have $ax + y - z = -(1 + 2a^2) < 0$, so by the previous lemma,

$$1 + 4\left(\left(1 + \frac{1}{2a^2}\right)\frac{1 + 4a^2}{2}\right)^{-s} f(s) < f(s, O) < 1 + 4\left(\frac{1 + 4a^2}{2}\right)^{-s} f(s),$$

so $f(s, O)$ converges at s if and only if $f(s)$ converges at s. □

Thus, it is sufficient to find the boundary of convergence for $f(s)$.

For a subtree U of Γ, let the *boundary* of U be the set

$$\partial U = \{\sigma \in \Gamma : \sigma \notin U, R_i\sigma \in U, i \in \{1, 2, 3\}\}.$$

Then, for any $U \subset U_3$ that contains the identity,

$$f(s) = \sum_{\sigma \in U} h(\sigma A)^{-s} + \sum_{\sigma \in \partial U} f_i(s, \sigma A),$$

where the i are chosen so that $R_i\sigma \in U$ – that is, if R_i gives descent from σA. We use the self similarity result, Lemma 3.5, to bound each $f_i(s, \sigma A)$, though a little more work is still required:

Lemma 3.7. *Let $X = (x, y, z)$ and let*

$$l_2(s, X) = \sum_{k=0}^{\infty}\left(\left(2a^2(z - y)k^2 + 2axk + \frac{y + z}{2}\right)^{-s} + \left(2a^2(z - y)k^2 + 2(ax + z - y)k + \frac{y + z}{2} + \frac{2ax - y + z}{2a^2}\right)^{-s}\right),$$

$$l_3(s, X) = l_2(s, (x, -y, z)),$$

$$l_1(s, X) = l_2(s, R_2X) + l_3(s, R_3X),$$

$$m_2(s, P) = \sum_{k=0}^{\infty}\left(\left(2a^2(z - y)k^2 + 2(ax + y - z)k + \frac{y + z}{2} - \frac{2ax + y - z}{2a^2}\right)^{-s} + \left(2a^2(z - y)k^2 + 2axk + \frac{y + z}{2}\right)^{-s}\right),$$

$$m_3(s, X) = m_2(s, (x, -y, z)),$$

$$m_1(s, X) = m_2(s, R_2X) + m_3(s, R_3X).$$

If R_i gives descent from X and $s > \frac{1}{2}$, then

$$l_i(s, X)f(s) < f_i(s, X) < m_i(s, X)f(s) + O(1).$$

Proof: Note that

$$f_2(s, X) = \sum_{k=0}^{\infty}\big(h((R_2R_1)^kX)^{-s} + f_3(s, R_3(R_2R_1)^kX) + h(R_1(R_2R_1)^kX) + f_3(s, R_3R_1(R_2R_1)^kX)\big),$$

and that

$$(R_2R_1)^kX = \big(x + 2ka(z - y), y + 2kax + 2k^2a^2(z - y), z + 2kax + 2k^2a^2(z - y)\big).$$

Applying Lemma 3.5 and noting that $s > \frac{1}{2}$ we get

$$l_2(s, X)f(s) < f_2(s, X) < O(1) + m_2(s, X)f(s).$$

By symmetry, $f_3(s, X) = f_2(s, (x, -y, z))$. Finally,

$$f_1(s, X) = h(X)^{-s} + f_2(s, R_2X) + f_3(s, R_3X),$$

which gives us the stated bounds for $f_1(s, X)$. □

Finally, let $U(H) = \{\sigma \in U_3 : h(\sigma A) < H\}$, and let

$$L(s, H) = \sum_{\sigma \in \partial U(H)} l_i(s, \sigma A),$$

$$M(s, H) = \sum_{\sigma \in \partial U(H)} m_i(s, \sigma A),$$

where the i are chosen so that R_i gives descent from σA. Then

$$L(s,H)f(s) < f(s).$$

Thus, if $L(s,H) > 1$, then $f(s)$ cannot converge, so $s < \alpha$. Note that $L(s,H)$ is a decreasing function in s for $s \in \left(\frac{1}{2},\infty\right)$, so there exists a unique $s_{L,H}$ such that $L(s_{L,H},H) = 1$. This gives us a lower bound on α.

The function $M(s,H)$ also decreases for $s \in \left(\frac{1}{2},\infty\right)$, and so has a unique solution $s_{M,H}$ to $M(s,H) = 1$. This gives us an upper bound on α. The details are similar to those found in [Baragar 03] and [Baragar 98]. Roughly, one can show that if $f(s)$ converges at s, then

$$\begin{aligned} f(s) &< M(s,H)f(s) + O(H^2), \\ 1 &< M(s,H) + O(H^2/f(s)). \end{aligned} \tag{3–3}$$

The problem is that $f(s)$ diverges at $s_{M,H}$, so the inequality does not make sense there. The solution is to derive an inequality similar to (3–3) that involves partial sums for $f(s)$.

By taking a large enough partial sum and $s < \alpha$, we can make the error term as small as we like, which gives us a contradiction if $s_{M,H} < s < \alpha$. Thus, $s_{M,H}$ is an upper bound for α.

To find the bounds in Table 1, we write a program that approximates $L(s,H)$ and $M(s,H)$. For the infinite sums in these functions, we use Euler–Maclaurin summation, as described in [Baragar 03, Section 4]. For the calculations shown in Table 1, we use $H = 10^5$ for $a < 2$; we use $H = 5 \cdot 10^5$ for $2 \le a < 4$; we use $H = 10^6$ for $4 \le a \le 8$; and we use $H = 10^7$ for $a \ge 9$.

ACKNOWLEDGMENTS

I would like to thank Michael Bennett, Peter Borwein, the Pacific Institute of Mathematical Sciences, and Simon Fraser University for their support and hospitality while this paper was being written. This research is supported, in part, by NSF grant DMS-0403686.

REFERENCES

[Baragar 98] A. Baragar. "The Exponent for the Markoff–Hurwitz Equations." *Pac. J. Math.* 182:1 (1998), 1–21.

[Baragar 03] A. Baragar. "Orbits of Curves on Certain K3 Surfaces." *Compositio Math.* 137:2 (2003), 115–134.

[Jenkinson and Pollicott 02] O. Jenkinson and M. Pollicott. "Calculating Hausdorff Dimension of Julia Sets and Kleinian Limit Sets." *Amer. J. Math.* 124 (2002), 495–545.

[Lax and Phillips 82] P. D. Lax and R. S. Phillips. "The Asymptotic Distribution of Lattice Points in Euclidean and Non-Euclidean Spaces." *J. Funct. Anal.* 46:3 (1982), 280–350.

[McMullen 98] C. T. McMullen. "Hausdorff Dimension and Conformal Dynamics III: Computation of Dimension." *Amer. J. Math.* 120:4 (1998), 691–721.

[Phillips and Sarnak 85a] R. Phillips and P. Sarnak. "On the Spectrum of the Hecke Groups." *Duke Math. J.* 52:1 (1985), 211–221.

[Phillips and Sarnak 85b] R. Phillips and P. Sarnak. "The Laplacian for Domains in Hyperbolic Space and Limit Sets of Kleinian Groups." *Acta Math.* 155:3–4) (1985), 173–241.

[Pignataro and Sullivan 1986] T. Pignataro and D. Sullivan. "Ground State and Lowest Eigenvalue of the Laplacian for Noncompact Hyperbolic Surfaces." *Comm. Math. Phys.* 104:4 (1986), 529–535.

Arthur Baragar, University of Nevada Las Vegas, Las Vegas, NV 89154-4020 (baragar@unlv.nevada.edu)

Received December 11, 2003; accepted in revised form November 23, 2005.